

**A&A manuscript no.**  
(will be inserted by hand later)

**Your thesaurus codes are:**  
11(11.05.1; 11.05.02; 11.06.1; 13.09.1; 12.03.3;)

**ASTRONOMY  
AND  
ASTROPHYSICS**  
October 11, 2018

# An Extremely Red $r^{1/4}$ Galaxy in the Test Image of the Hubble Deep Field South<sup>☆</sup>

T. Treu<sup>1,2</sup>, M. Stiavelli<sup>1,2,6</sup>, A. R. Walker<sup>3</sup>, R. E. Williams<sup>2</sup>, S. A. Baum<sup>2</sup>, G. Bernstein<sup>4</sup>, B. S. Blacker<sup>2</sup>, C. M. Carollo<sup>5\*\*</sup>, S. Casertano<sup>2,6</sup>, M. E. Dickinson<sup>2</sup>, D. F. Demello<sup>2</sup>, H. C. Ferguson<sup>2</sup>, A. S. Fruchter<sup>2</sup>, R. A. Lucas<sup>2</sup>, J. Mackenty<sup>2</sup>, P. Madau<sup>2</sup>, and M. Postman<sup>2</sup>

<sup>1</sup> Scuola Normale Superiore, Piazza dei Cavalieri 7, I56126, Pisa, Italy; treu@cibs.sns.it, mstiavel@astro.sns.it

<sup>2</sup> Space Telescope Science Institute, 3700 San Martin Dr., 21218 MD, U.S.A.; treu@stsci.edu, mstiavel@stsci.edu, wms@stsci.edu

<sup>3</sup> Cerro Tololo Inter-American Observatory, NOAO, Casilla 603, La Serena, Chile; awalker@noao.edu

<sup>4</sup> University of Michigan, Dept. of Astronomy, 830 Dennison Building, Ann Arbor, MI 48109, U.S.A.

<sup>5</sup> Johns Hopkins University, 3701 San Martin Dr., 21218 MD, U.S.A.

<sup>6</sup> On assignment from the Space Science Department of the European Space Agency

Received / Accepted

**Abstract.** We report the serendipitous discovery of an extremely red object in the Hubble Deep Field South (HDFS) Test NICMOS (Near Infrared Camera and Multi Object Spectrograph) field of view. The object is resolved in the NICMOS image and has a light profile very well described by an  $r^{1/4}$  law with effective radius  $r_e = 0''.20 \pm 0.05$  and  $H_{AB} = 21.7 \pm 0.1$  magnitudes. In contrast, the galaxy is undetected in the R and I band ground based images taken at the CTIO 4 m Blanco Telescope, giving a lower limit to the color of  $(R-H)_{AB} > 3.9$  and  $(I-H)_{AB} > 3.5$  at the 95 % confidence level. The colors of a range of synthetic galactic spectra are computed, showing that the object is likely to be an “old” elliptical galaxy at redshift  $z \gtrsim 1.7$ . Alternatively the colors can be reproduced by an “old” elliptical galaxy at somewhat lower redshift ( $\gtrsim 1$ ) with significant amount of dust, or by a younger galaxy at higher redshift. This object represents a very interesting target for future VLT observations.

**Key words:** Galaxies: elliptical and lenticular, cD—Infrared: galaxies—Galaxies: formation—cosmology: observations—early universe

## 1. Introduction

The joint effort of the Hubble Space Telescope (HST) and large ground based telescopes in the last few years

*Send offprint requests to:* T. Treu

<sup>☆</sup> Based on observations collected with the NASA/ESA HST, obtained at the STScI, which is operated by AURA, under NASA contract NAS5-26555 and at the CTIO, NOAO, which is operated by AURA, under cooperative agreement with the NSF.

<sup>\*\*</sup> Hubble Fellow

*Correspondence to:* T. Treu

has produced a real breakthrough in our understanding of the history of formation and evolution of galaxies. Deep photometric multicolor imaging such as the Hubble Deep Field (HDF, Williams et al. 1996) together with spectroscopic information (e.g., Lilly et al. 1995; Steidel et al. 1996; Lowenthal et al. 1997) have started to sketch a sort of cosmic timetable that provides important constraints to theories for the formation of cosmic structure (Steidel et al. 1998; Baugh et al. 1998). Besides global properties (Madau et al. 1996), the superb resolution of the HST allows us to study the evolution of different morphological types separately, in particular to clarify the history of elliptical galaxies (E/S0). The intermediate redshift spectroscopic data (e.g. van Dokkum et al. 1998) suggest a mostly passive evolution of old stellar populations that seems to be confirmed by photometric studies at higher redshift (Schade et al. 1997; Driver et al. 1998).

To push the investigation to redshift significantly greater than 1, infrared (IR) photometry (corresponding to optical rest-frame emission) is needed (e.g. Maoz 1997; Dickinson 1998). The extremely red objects with  $(R-K) > 5$  (equivalently  $(R-K)_{AB} > 3.3$ ) found with IR surveys are generally thought to be high redshift elliptical galaxies (e.g., Hu & Ridgway 1994; Spinrad et al. 1997). However, due to their subarcsecond sizes, HST is needed to explore in detail the morphology of these objects (Graham & Dey 1996).

In this Letter we report the discovery of a “R-H dropout” (Figs. 1 **a**, **b** and **c** in the HDFS test image. The morphology, the size and the colors (R-H and I-H) strongly suggest the object to be an “old” elliptical galaxy (or bulge-dominated object) at  $z \gtrsim 1.7$  and therefore with a very high formation redshift ( $z_f$ ), somehow similar to the “old” red galaxy found by Spinrad et al. (1997) at redshift  $z = 1.55$ . Many extremely red objects have been found in the last years (see e.g. Elston et al. 1988; Dey et al. 1995;

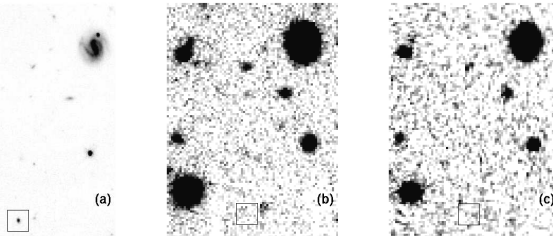


**Fig. 1.** **a.** HST NICMOS F160W “drizzled” image (7680 s). **b.** CTIO 4m R (3000 s). **c.** CTIO 4m I (2800 s). North is up and East is left in the CTIO exposures, while the NICMOS image is slightly rotated. The frames are  $\approx 35'' \times 45''$ . The boxes are centered on the position of the galaxy.

Moustakas et al. 1997; Stanford et al. 1997) using ground based IR photometry, thus with poor morphological information. At the opposite, the object we present in this Letter, thanks to the HST angular resolution, is resolved and we can measure the light profile and the effective radius (similar objects are being detected with NICMOS, e.g. McCarthy et al. 1998, but the luminosity profile has not been measured). The luminosity profile is well described by an  $r^{1/4}$  law. Models with dust are also considered to explain the extremely red colors, given the growing evidence for significant amounts of dust in high redshift galaxies (Soifer et al. 1998; Cimatti et al. 1998). The Hubble constant is assumed to be  $100 h \text{ km/s/Mpc}$ , with  $h = 0.65$  where needed.

## 2. Photometry

During the HDFS test program (Williams et al. 1997) images of the candidate HDFS field were taken with the F160W filter of the Near Infrared Camera and Multi Object Spectrometer (NICMOS) on board the HST (Fig. 1 **a**), and in the optical R band (Fig. 1 **b**) with the 4m Blanco Telescope at the Cerro Tololo Inter-American Observatory (CTIO). Follow up I band photometry was obtained on May 13 1998 at the same telescope (Fig. 1 **c**).

### 2.1. The Infrared NICMOS Imaging

Twelve NICMOS Camera 3 (NIC3) images of the field were taken in MULTIACCUM mode (640 s each). The images were obtained at six different pointings in order to correct for bad pixels and to recover the information lost to undersampling of NIC3 (approximately  $0''.2$  pixel size).

The “pedestal”, an unpredictable bias that affects the NICMOS images (see the NICMOS Image Anomalies web page at URL [www.stsci.edu/ftp/instrument\\_news/NICMOS/nicmos\\_anomalies.html](http://www.stsci.edu/ftp/instrument_news/NICMOS/nicmos_anomalies.html)), was removed using the Pedestal Estimation Software by R. P. van der Marel, and scripts developed by one of us (MED). The dithered images were combined on a subsampled grid ( $0''.1$  pixel size, shown in Fig. 1 **a**) using the DRIZZLE IRAF/STSDAS

task (Fruchter & Hook 1998). A bad pixel and cosmic ray mask was obtained by using the IRAF/STSDAS package DITHERII.

The object appears resolved on the final drizzled images, but to be sure that this was not an artifact of the reduction procedure we performed a  $\chi^2$  test on the single calibrated frames. For each image we measured the FWHM along the x and y axis of the galaxy and the two nearby stars (using the MIDAS command CENTER/GAUSS). We estimated the error on the FWHM to be the standard deviation of the values measured on the different frames (about  $0''.04$ ). The reduced  $\chi^2$  of the values with respect to their average is therefore 1 (by definition). The reduced  $\chi^2$  of the measured FWHMs computed with respect to the average stellar FWHM is  $\chi^2 = 11.1$ , showing that the object is resolved.

The luminosity profile of the galaxy (Fig. 2) was obtained by fitting elliptical isophotes to the image with a modified version of the MIDAS command FIT/ELL3 specifically designed to deal with undersampled images (Møller, Stiavelli & Zeilinger, 1995).

In order to fit a luminosity profile law to the data point it is crucial to determine the PSF very accurately. An unexpected deformation of the NICMOS dewar pushed NIC3 out of the range reachable by the focusing device (Pupil Alignment Mechanism) and therefore NIC3 is always somewhat out of focus. Thermal breathing of the instrument (that is significant during long exposures) and the combination of multiple dithered exposures add further uncertainty and broadening to the PSF. For these reasons the stars in the field are a better approximation of the real PSF than the PSFs obtained with Tiny Tim 4.4; the main residual difference may be caused by position-dependent features of the NIC3 PSF. In order to have an estimate of the errors due to the PSF, we fitted the profile with different PSFs: the two nearest stars and two “synthetic” ones computed as follows. A PSF was calculated using Tiny Tim 4.4 (using a 15 mas jitter) on a subsampled grid ( $0''.02$  pixel size) in the same position of a star in the HDFS test image. It was then rebinned to the scale of the drizzled image in order to obtain a PSF centered in the same sub-pixel of the real star. Under the assumption that the “true” PSF ( $S$ ) is the convolution of the Tiny Tim PSF ( $T$ ) with a position independent broadening function ( $B$ ) due mostly to the breathing of NICMOS and the drizzling of the single dithered images, we derived the function  $B$  using the MIDAS fourier transform commands. The broadening functions  $B_1$  and  $B_2$  were derived for the two nearest stars. Using a Tiny Tim PSF ( $T_g$ ) centered on the galaxy center and the broadening functions we obtained two “synthetic stars”  $\text{syn1} = T_g \circ B_1$  and  $\text{syn2} = T_g \circ B_2$ . As we were interested in checking the robustness of the results with respect to PSF uncertainties, we performed the fits using both the two real stars and the two “synthetic” stars.

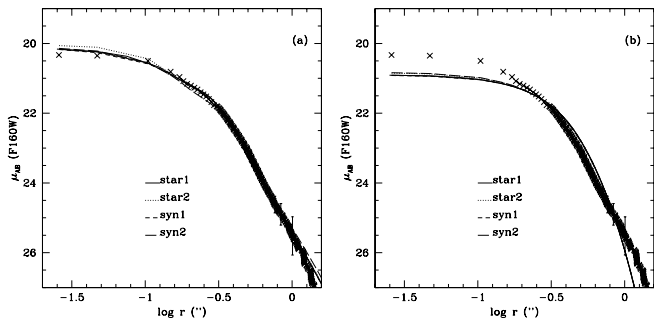


**Fig. 2.** IR (F160W) luminosity profile of the galaxy (crosses). The PSF-convolved best-fit  $r^{1/4}$  (a) and exponential (b) profiles are shown. Only a few error bars are shown for clarity. Four different fits are obtained by using different PSF profiles as described in the text.

We fitted an  $r^{1/4}$  law to the isophotal profile, using a code described, e.g., by Carollo et al. (1997). The fit obtained with the four PSFs are in excellent mutual agreement and reproduce the data very well (Fig. 2 a). If an exponential profile component is added, the best fit is obtained for a very small exponential component and a practically unchanged  $r^{1/4}$  component. At the opposite, an exponential disk by itself gives a poor description of the profile (Fig. 2 b). The photometric parameters were also determined with a two-dimensional fit code, described in Treu et al. (1998). The total error is mainly due to residual PSF mismatches, to the specific technique (profiles or 2D fit), and to errors in the sky subtraction. The PSF and the technique dependent uncertainties can be estimated from the scatter of all the photometric parameters derived, while the sky-subtraction error has been estimated by varying the sky level ( $\approx 15\%$  in  $r_e$  and  $\approx 0.1$  mag in  $m$ ). The average values of the effective radius and magnitude, obtained with different techniques, models and PSFs, are respectively  $r_e = 0''.20 \pm 0.05$  and  $m = 21.7 \pm 0.1$ .

## 2.2. The R and I ground-based photometry

Ten dithered R band exposures (300 s each) were obtained with the Prime Focus CCD (PFCCD) Imager at the CTIO Blanco 4m telescope on May 2 1997, using the detector SITe 2K #6. The night was photometric with seeing  $1''.2$ . The same field was observed in the I band on May 13 1998 (unfortunately almost Full Moon was present) with the Tyson-Bernstein Mosaic Imager. CCD #3, also a SITe 2K, was pointed at the PFCCD field, obtaining  $14 \times 200$  s dithered exposures. The night was photometric, with  $1''.0$  seeing. The images were reduced and combined in standard way using IRAF.

The photometric calibration of the R band was done by bootstrapping the photometry from a 0.9m to the 4m image. Three relatively bright ( $I \sim 18$ ) stars near the NICMOS position were calibrated on the I-band frame by reference to seven stars in Landolt (1992) SA 107. Both were also checked with the nominal zeropoints from the instrument manuals. The accuracy of the calibration is about 0.1 mag, which is good enough for our purposes.

The galaxy, which is quite evident on the NICMOS images, is undetected in both the R and I CTIO image (Figs. 1 b and c). Thus we can only set an upper limit to the R and I band luminosities. The nearest detected source is at  $\approx 3''$  on the R band image. The limiting magnitudes, computed by measuring the sky noise ( $\delta K$ ) and correcting the resulting flux for the seeing losses, are  $m_R > 25.9$  and  $m_I > 24.7$  AB mag at the two-sigma level.

A more accurate limit can be given by considering the statistical distribution of the counts on the detector for a given source of intensity  $I_0$  and a given background of zero average and variance  $\delta K^2$ . The 95 % confidence level (CL) limit is  $m_R > 25.6$  and  $m_I > 25.2$  ABmag. The limits on the color are therefore  $(R-H)_{AB} > 4.3$  and  $(I-H)_{AB} > 3$ , at the two-sigma level, considering only the sky variance, but  $(R-H)_{AB} > 3.9$  and  $(I-H)_{AB} > 3.5$ , at the 95 % CL with the more accurate algorithm.

## 3. Identification

The morphology and the IR light profile suggest that the object is a high redshift “old” elliptical galaxy. But the strongest clues in favor of a high redshift elliptical galaxy are the colors. To better constrain this identification we have computed the  $(R-H)_{AB}$  and  $(I-H)_{AB}$  colors of a set of synthetic spectra of single burst elliptical galaxies (Bruzual & Charlot, 1993; GESSEL 96 version) as a function of redshift. A standard Salpeter IMF and metallicities  $Z = Z_\odot$  and  $Z = 0.2Z_\odot$  have been used. The lower metallicity has been selected to be representative of the low metallicity environment that one could expect to find in primordial stellar populations. In Figs. 3 a and b the contour plots of  $(R-H)_{AB}$  and  $(I-H)_{AB}$  (isochromes) as a function of redshift and age of the synthetic galaxy are shown. For each given redshift the galaxy age has to be less than the age of the Universe, which is overplotted as thin lines for two different values of the cosmological parameters  $\Omega$  and  $\Omega_\Lambda$ . In practice, only the points above the maximum of the lower branches of the two isochromes (I and R), and below the thin line for the selected cosmology, are consistent with the observed colors. As can be seen, the colors support the identification as an “old” elliptical galaxy at redshift  $\gtrsim 1.7$  for the solar metallicity models. The lower limit in redshift is even more stringent if we consider low metallicity spectra, because the Balmer Jump is intrinsically shallower. A redshift  $z \gtrsim 1.7$  would also give an effective radius in the usual range for elliptical galaxies ( $\gtrsim 1$  kpc). The colors are well reproduced also for much higher redshift ( $\sim 7-15$ ).

A significant content of dust (which can be found in high redshift star-forming galaxies, see e.g. Soifer et al.

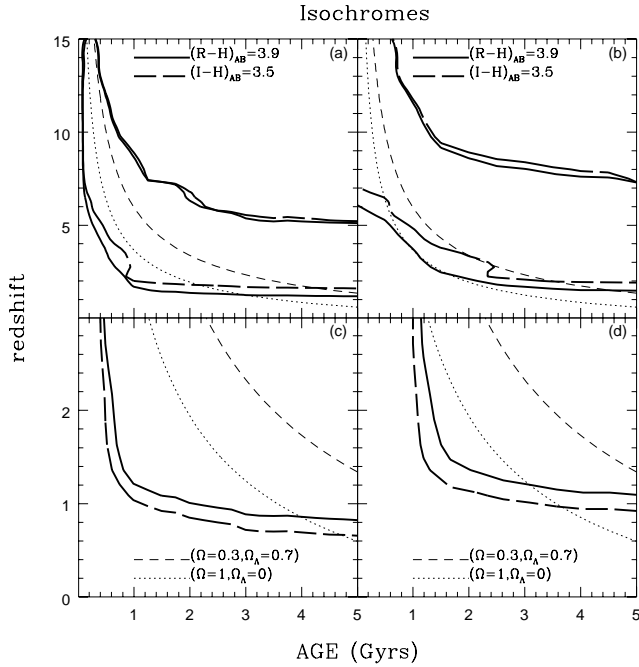


**Fig. 3.** **a.** Contour plot (thick lines) of the  $(R-H)_{AB}$  (solid) and  $(I-H)_{AB}$  (dashed) colors (isochrone) as a function of redshift and age of an elliptical galaxy, computed using synthetic spectra of solar metallicity. The age of the Universe as a function of redshift is overplotted as thin lines for two different cosmological models. See text for discussion and details. **b.** As in **a** but the models have metallicity  $Z = 0.2Z_{\odot}$ . **c.** As in **a** but the spectra have been reddened for dust ( $A_V = 0.5$ , see text). **d.** As in **c** but the models have metallicity  $Z = 0.2Z_{\odot}$ .

1998, Cimatti et al. 1998) could redden the colors of a given galactic spectrum and redshift. For this reason, the same isochrones were computed after reddening the spectra for dust absorption following the extinction law given by Cardelli et al. (1989) with  $A_V = 0.5$ ,  $A_V = 3.1E(B-V)$ . In Figs. 3 (c) and (d) the isochrones are shown in the low redshift (0–3) range. The colors are now reproduced by lower redshift models ( $z \gtrsim 1$ ), and therefore the object could be a high redshift “old” elliptical galaxy with significant dust content.

#### 4. Conclusions

The object, that has been selected as an “R-H dropout” in the test image of the HDFS, is clearly resolved on the NICMOS image and shows an  $r^{1/4}$  law profile with an effective radius of  $0''.20$ . The colors  $(R-H)_{AB}$  and  $(I-H)_{AB}$  are well reproduced by synthetic models of “old” elliptical galaxies at redshift  $z \gtrsim 1.7$  or at higher redshift (up to  $\sim 15$ ) by younger ones (Sect. 3), implying therefore a very high formation redshift. Alternatively it could be a lower redshift ( $z \gtrsim 1$ ) elliptical galaxy with a significant amount of dust. High redshift clusters

of galaxies have been photometrically identified in the vicinity of QSOs (Francis et al. 1996; Steidel et al. 1998). Therefore this galaxy may possibly be a companion to the QSO J2233-60, which is located  $\approx 8'$ , i.e.  $\approx 2h^{-1}$  Mpc (physical distance) from the HDFS NIC3 field. This identification would then lead to  $z \approx 2.22$  compatible with the colors and size that we have observed. At this redshift,  $H_{AB}=21.7$  would imply an absolute magnitude  $M_V = -22.7$  ( $\Omega=1$ ,  $\Omega_{\Lambda}=0$ ) and  $M_V = -23.3$  ( $\Omega=0.3$ ,  $\Omega_{\Lambda}=0.7$ ) which are normal for a 1.5 Gyr-old elliptical<sup>1</sup>.

Further spectroscopic and photometric investigation are needed to measure the redshift, to study in detail the stellar population, to clarify the role of dust, and to identify possible high redshift companions. The faintness of the object though, makes it extremely hard to measure the redshift with 4m class telescopes, while it will be feasible in a few hours with the ISAAC spectrograph at the VLT (see the VLT-ISAAC web page [www.eso.org/instruments/isaac](http://www.eso.org/instruments/isaac)).

*Acknowledgements.* The authors would like to thank R. P. van der Marel, who developed the Pedestal Estimation Software used for the pedestal subtraction. TT would like to thank Prof. G. Bertin for carefully reading the manuscript.

#### References

Baugh C., Cole S., Frenk C., Lacey C. 1998, ApJ, 498, 504  
 Bruzual A. G., Charlot S. 1993, ApJ, 405, 538  
 Cardelli J., Clayton G., Mathis J. 1989, ApJ, 345, 245  
 Carollo C. M., Franx M., Illingworth G. D., Forbes D. A. 1997, ApJ, 481, 710  
 Cimatti A., Andreani P., Röttgering H., Tilanus R. 1998, Nature, 392, 895  
 Dey A., Spinrad H., Dickinson M. E. 1995, ApJ, 440, 515  
 Dickinson M. E., 1998, preprint (astro-ph/9802064v2)  
 Driver S. P., Fernández-Soto A., Couch W. J., Odewhan S. C., Windhorst S. C., Phillipps S., Lanzetta K., Yahil A. 1998, ApJ, 496, L93  
 Elston R., Rieke G. H., Rieke M. J. 1988, ApJ, 331, L77  
 Fruchter A. S., Hook R. N. 1998, submitted to PASP  
 Francis P. J. et al. 1996, ApJ, 457, 490  
 Graham J. R., Dey A. 1996, ApJ, 471, 720  
 Hu E. M., Ridgway S. E. 1994, AJ, 107, 1303  
 Landolt A. U. 1992, AJ, 104, 340  
 Lilly S. J., Tresse L., Hammer F., Crampton D., Le Févre O. 1995, ApJ, 455, 108  
 Lowenthal J. D. et al. 1997, ApJ, 481, 673  
 Madau P., Ferguson H. C., Dickinson, M. E., Giavalisco M., Steidel C. C., Fruchter A. 1996, MNRAS, 283, 1388  
 McCarthy P., Yan L., Storrie-Lombardi L., Weymann R. J., 1998, in: NICMOS and the VLT, ESO Conference Workshop Proceedings 55, W. Freudling and Richard Hook eds.  
 Maoz D. 1997, ApJ, 490, 135  
 Møller P., Stiavelli M., Zeilinger W. 1995, MNRAS, 276, 979

<sup>1</sup> A 1.5 Gyrs synthetic spectrum (Bruzual & Charlot 1993) of solar metallicity was used to compute the K-correction and the filter transformation.

Moustakas L. A., Davis M., Graham J. R., Silk J., Peterson B. A., Yoshii Y. 1997, ApJ, 475, 445

Schade D., Barrientos L., López-Cruz O. 1997, ApJ, 477, L17

Soifer B. T., Neugebauer G., Franx M., Matthews K., Illingworth G. D. 1998, ApJ, 501, L171

Spinrad H., Dey A., Stern D., Dunlop J., Peacock J., Jimenez R., Windhorst R. 1997, ApJ, 484, 581

Stanford S. A., Elston R., Eisenhardt P. R., Spinrad H., Stern D., Dey A. 1997, AJ, 114, 2232

Steidel C. C., Giavalisco M., Dickinson M. E., Adelberger K. L., 1996 ApJ, 462, L17

Steidel C. C., Adelberger K. L., Dickinson M. E., Giavalisco M., Pettini M., Kellogg M. 1998, ApJ, 492, 428

Treu T., Stiavelli M., Casertano S., Møller P., Bertin G. 1998, submitted to MNRAS

van Dokkum P., Franx M., Kelson D., Illingworth, G. D. 1998 to be published in ApJL, 504

Williams R. E. et al. 1996, AJ, 112, 1335

Williams R. E. et al. 1997, AAS, #191.8508